International Journal of Engineering & Technology, 6 (2) (2017) 21-28

SPC

International Journal of Engineering & Technology

Website: www.sciencepubco.com/index.php/IJET
doi: 10.14419/ijet.v6i2.7418
Research paper

Stress and strain distributions in the human hand-arm system using finite element analysis

Surajudeen Adewusi [1] *, Marc Thomas [2]

[1] Mechanical Engineering Department, Jubail University College, Royal Commission for Jubail & Yanbu P.O. Box 10074 Jubail Industrial City 31961, Kingdom of Saudi Arabia
[2] Research Laboratory in Machinery, Process and Structural Dynamics (DYNAMO), Mechanical Engineering Department, Ecole de Technologie Superieure, 1100 Notre-Dame Street West, Montreal, Quebec, Canada, H3C 1K3
**Corresponding author E-mail: adewusis@ucj.edu.sa, adedotun1@yahoo.com*

Abstract

This study presents stress and strain distributions in the human hand-arm system exposed to vibrations using finite element (FE) models. Frequency weightings at shoulder, elbow, wrist and palm based on stress and strain distributions were proposed. The stress/strain-based frequency weightings around the shoulder and elbow are comparable with that reported in the International Organization for Standardization ISO 5349-1, Mechanical vibration and shock– Measurement and evaluation of human exposure to mechanical vibration – part 1: General Requirements, 2001. However, stress/strain-based frequency weightings around the palm and wrist are different above 20 Hz from the weighting reported by the International Standard Organization. This study suggests the need for different frequency weightings for the assessment of the potential injury of different components of the hand-arm vibration syndrome.

Keywords: *Hand-Arm Vibrations; Finite Element Model; Resonant Frequencies; Stress/Strain Distributions, Frequency Weightings.*

1. Introduction

Epidemiological studies have shown that operators of hand-held power tools who are exposed to prolonged hand-transmitted vibration (HTV) developed hand-arm vibration syndrome (HAVS) such as vascular, sensorineural and musculoskeletal disorders [1-3]. These disorders could be classified into two major groups namely (1) vibration-induced white fingers (VWF), and (2) pain in the arms and joints (musculoskeletal disorder). In order to understand injury mechanism and mitigate HAVS, researchers have been studying biodynamic responses of the human hand-arm system exposed to vibration in terms of mechanical impedance and vibration transmissibility [4-8], and assessment of potential injury associated with prolonged exposure to HTV [9], [10]. These research efforts have resulted to several national and international standards [11] on how to measure, assess and mitigate HTV and the associated potential injuries. However, some studies have presented conflicting results between injury assessments (particularly for the vibration-induced white fingers) based on the current ISO 5349-1 guidelines and frequency weighting [11] and epidemiological studies [12], [13]. A recent study [14] have also shown that a single weighting proposed in [11] cannot account for the frequency-dependence of all factors (e.g. psychophysical, physiological, vibration magnitude, contact conditions, individual susceptibility, posture) contributing to hand-arm injury. Furthermore, some studies have suggested alternative frequency weightings for potential hand-arm injury assessment for different parts of the hand-arm [15-18]. Consequently, the working group of ISO Technical Committee ISO/TC 180/SC 4 on Human Exposure to Mechanical Vibration and Shock has evaluated other alternative frequency weightings to improve the current frequency weighting defined in ISO 5349-1 butno better single weighting was found for the assessment of injury risk for HAVS [19].

One of the alternative frequency weightings considered in the study [19] was derived from the vibration power absorption of the finger-hand-arm obtained from lumped-parameter models of the human hand-arm system [16]. The majority of the reported lumped-parameter hand-arm models [5], [16], [20] were derived from Driving-Point Mechanical Impedance (DPMI) responses and considered the fingers and palm, but the hand-arm posture and anatomical structure were not considered. Moreover, the masses of the bones and muscles/tissues of the palm-wrist-forearm substructures were lumped together to form a rigid member in the model. Hand-arm models derived from DPMI may not yield reliable distributed biodynamic responses at other locations (wrist, elbow and shoulder). In order to improve the reliability of biodynamic responses at other locations, some studies presented biomechanical models of the hand-arm system that are derived from both the DPMI and transmissibility responses with the consideration of hand-arm postures and anatomical structure [21, 22]. To the best knowledge of the authors, the muscles and bones of the arms are combined in all the reported lumped-parameter models of the human hand-arm system. These lumped-parameter models may not yield accurate stress and strain distributions.

Finite element (FE) models already used to evaluate the injury risk of the lumber vertebra of a seated human body exposed to vertical vibration by studying the stress distributions [23]. Similarly, hand-arm potential injury risk may be related to stressing and/or strain distribution, which can be obtained from FE models of the hand-arm system once calibrated. However, due to the complexity of the human hand-arm system, only limited studies presented two-dimensional (2D) FE models of the fingertip [24], [25]. Very recent studies presented 2D FE models into hand-arm system in the bent-arm and extended arm postures for modal analysis [26], [27]. These

FE models could be used to study stress and strain distributions and to derive stress/strain-based frequency weightings.

This study presents stress and strain distributions in different sub-structures of the hand-arm and stress/strain-based frequency weightings using 2D finite-element models of the human hand-arm system in two postures: the extended arm and bent-arm postures. Von-Mises equivalent stress/strain distributions in different sub-structures of the hand-arm models as a function of frequencies are examined and stress-based frequency weightings for the palm, wrist, elbow and shoulder are derived for comparison with the ISO 5349-1 [11] and other reported frequency weightings.

2. Methods

2.1. Finite element models

2D FE models of the human hand-arm, which consist of the palm (carpals bones lumped together), forearm (radius and ulna bones), upper-arm (humerus bone), muscles/tissues, wrist, elbow and shoulder joints and the trunk in the extended arm and bent-arm postures are presented in Figure 1(a) and Figure 1(b), respectively. For simplicity, the fingers are not considered since a few studies have presented the 2D FE model of the fingertip studies [24], [25]. The humerus, radius and ulna bones consist of the cortical (hard) bone around the middle-span and trabecular (soft) bones at the ends. The bones are assumed to be in contact at joints and then held together by muscles/tissues. The mean anthropometric dimensions (Table 1) of the hand-arm of 6 subjects who participated in a laboratory measurements of vibration transmissibility responses of the human hand-arm system exposed to z_h-axis vibration [7], and the reported bone dimensions were used to develop the FE models in ANSYS. The responses are observed at four different locations around the palm (*X1*), wrist (*X2*), elbow (*X3*) and shoulder (*X4*) as shown on Figure 1. It should be mentioned that the extended arm model (Figure 1(a)) is similar to the posture assumed by the subjects during experimental measurements of transmissibility, described in section 2.2 while the bent-arm model (Figure (1b)) has elbow angle of 130^o instead of 90^o elbow angle posture of the subjects during the experimental measurements; this is to simplify the 2D FE model in the bent-arm posture. The posture of the bent-arm FE model is still within the recommended posture in the ISO10068 Standard [28]. The recommended posture in the standard consists of elbow angle between65^o and 165^o. Although the recommended posture in the ISO 10068 standard corresponds to the bent-arm posture, the extended arm posture is also considered because it is impossible to maintain the bent-arm posture for the operation of heavy hand-held power tools, e.g. road breakers. The shoulder boundary condition is such that it permits the motion of the shoulder by the inclusion of the trunk. All the components of the trunk (spines, scapular, abdomen, etc.) are lumped together as shown in Figure 1 to simplify the models since stresses and strain in the trunk are not required for this study. Fixed boundary condition is applied at the pelvis only to allow motion of the trunk and hence the shoulder.

The ranges of the reported values for the mechanical properties of cortical and trabecular bones, and muscles/tissues [29-31], as summarized in Table 2, are used for the FE simulations using ANSYS. Plane182 element type is used for the tissues/muscles since this element type has plasticity, hyper-elasticity, stress stiffening, large deflection, and large strain capabilities. Other components are represented with Plane183 element type, which is good for modeling irregular shapes. The FE analysis was performed in two steps using ANSYS. The first was the harmonic analysis of the models where an excitation force of 50 N in the z_h-axis direction was applied at the palm side. It should be noted that the *x*- and *y-axis* in ANSYS correspond to the z_h- and y_h-axis, respectively, of the hand-arm coordinate system defined in ISO 5349-1 [11]. The Rayleigh damping coefficients was estimated from the damping ratios associated with resonant frequencies obtained from Operational Modal Analysis using Auto-regressive Moving Average and those estimated from prominent peaks in the low and high-frequency regions of the measured transmissibility response graphs [7] using half-power concept.

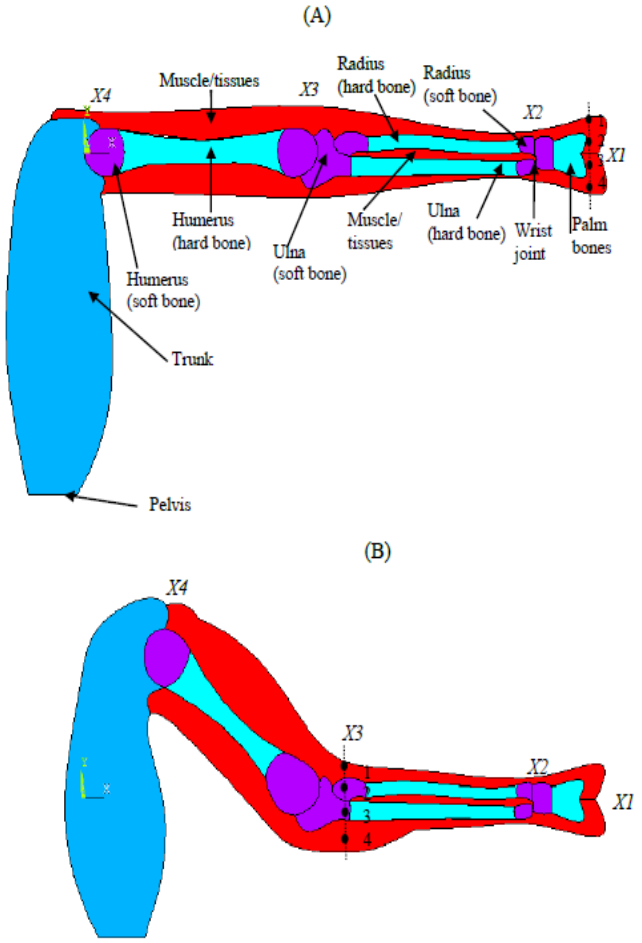

Fig. 1: FE Model of the Human Hand-Arm; (A) Extended Arm Posture; (B) Bent-Arm Posture.

Table 1: Dimensions of the Hand-Arm of Six Subjects

Hand-arm length and projected dimensions on a plane			
Parameters	Ranges	Mean	STD
Age (years)	26 - 53	36.5	11.33
Height (cm)	171 - 180	174.0	0.02
Weight (kg)	61 - 86	72.2	9.87
BMI	20.4 - 28.7	23.8	3.13
Hand length (cm)	17 - 20.5	18.4	1.20
Hand width at thumb (cm)	9.5 - 12.0	10.9	0.86
Hand width at metacarpal (cm)	7.0 - 8.5	7.5	0.63
Hand thickness (cm)	2.0 - 3.7	2.9	0.55
Wrist width (cm)	5.1 - 5.9	5.5	1.04
Forearm width (cm)	8.0 - 10.0	8.9	2.53
Elbow width (cm)	7.8 - 9.7	8.4	2.22
Forearm length (cm)	24.0 - 28.5	26.0	1.58
Upper arm width (cm)	8.9 - 10.5	9.0	3.13
Upper arm length (cm)	23.0 - 32.0	28.5	2.35

Table 2: Mechanical Properties of the Components of the Human Hand-Arm System

	Cortical bone	Trabecular bone	Muscles/ tissues
Young Modulus (MPa)	7230 - 17000	43.6 - 1060	345 - 888
Poisson ratio	0.3	0.3	0.3
Density (kg/cm^3)	1.5 – 2.0	1.0 – 7.0	0.75 – 1.2

2.2. Model calibration

It is well-known that the mechanical properties of the human muscles/tissues depend upon hand force. The FE models were calibrated by comparing the resonance frequencies obtained from the harmonic responses of the models with those derived from experimental vibration transmissibility responses [7]. This was achieved by simulating harmonic responses of the models in ANSYS starting with the estimated Rayleigh damping coefficients, and the lower values of the mechanical properties presented in Table 2. The harmonic analysis in ANSYS was performed and responses are computed at four different locations *X1*, *X2*, *X3* and *X4* as shown on Figure 1. Since responses may vary along the vertical direction (y_h-axis) at each of the four locations (*X1* – *X4*), the average of the responses at four points (1-4) along the vertical dotted lines as indicated on Figure 1 was computed.

The Rayleigh damping coefficients and mechanical properties was then slightly varied until the frequencies corresponding to peak of the harmonic responses from ANSYS are comparable with those derived from the analysis of experimental vibration transmissibility responses of the human hand-arm system reported in [7]. The hand-arm resonant frequencies for the bent-arm and extended arm postures were obtained from measured responses using two methods: (1) Operational Modal Analysis using Auto-regressive Moving Average of the acceleration signals, and (2) peaks in the transmissibility responses. For the extended arm model, the final mechanical properties obtained from the calibration of FE models are: Young Moduli for cortical bone, trabecular bone and muscles/tissues are 7230, 43.6 and 10.2 MPa, respectively. The corresponding densities are 2000, 700 and 750 kg/m^3. These mechanical properties were then used for modal analysis to determine the mode shapes of the FE models of the hand-arm for both postures. Details procedures and results for the calibration of the FE models have been published [26 and 27].

2.3. Stress and strain analysis

The distributions of stress and strain in the hand-arm models at some of the observed resonant frequencies are obtained from the FE analysis in ANSYS to study the regions of maximum stress and strain. Von-Mises equivalent stress and strain analysis in ANSYS was used. The changes in the stress and strain with frequency at four locations (*X1*, *X2*, *X3* and *X4*) corresponding to the palm, wrist, elbow and shoulder along the horizontal direction (z_h-axis), where harmonic responses were observed, are also obtained. The stress and strain at the four locations are normalized to obtain stress- and strain-based frequency weightings, which are then compared with some of the frequency weightings investigated by Pitts et al. [19]. The frequency weighting was obtained from normalized stress and strain as recommended in [17] such that:

$$\sigma_n(f) = 0.958\frac{\sigma(f)}{\sigma_{max}} \quad (1)$$

Where $\sigma_n(f)$ is the normalized stress/strain at frequency *f*, $\sigma(f)$ is the stress/strain at frequency *f*, σ_{max} is the maximum stress and 0.958 is the maximum weight of the frequency weighting reported in ISO 5349-1 [11] at 12 Hz.

3. Results and discussion

3.1. Stress and strain distributions in the human hand-arm at different frequencies

Figure 2 presents the distribution of Von-Mises equivalent stress for the extended arm model, while Figure 3 presents the strain distribution. Figure 4 presents the variations in stress and strain with change in frequency around the palm, wrist, elbow and shoulder.

Figure 2 shows that high stress is mostly developed in the bone structures of the extended arm and Figure 3 shows that strain is mostly developed in the muscles/tissues. The general trend is that stress and stain decreases with increase in frequency, as shown by the values of the color bar. Furthermore, the location of stress and strain concentration moves from the shoulder at low frequency towards the palm at high frequency. Below 12 Hz, high stress is developed in the humerus bone and high strain is developed around

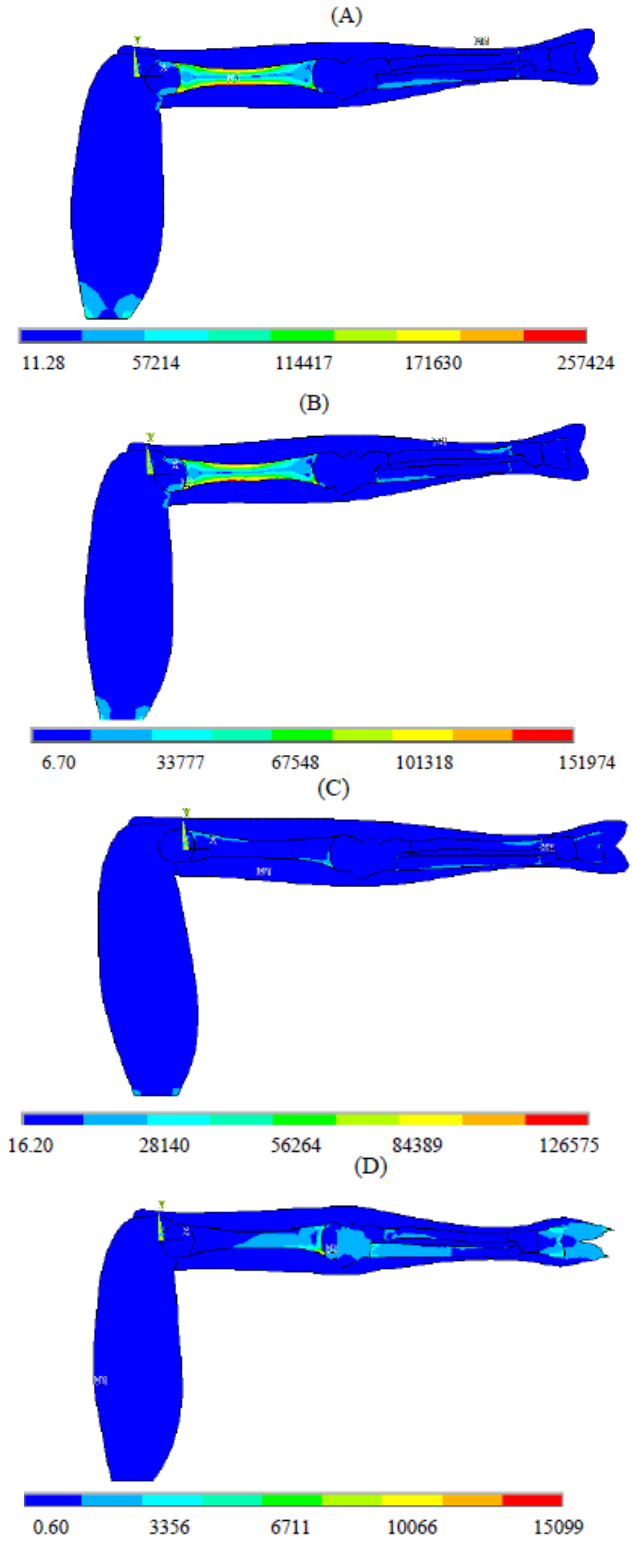

Fig. 2: Stress Distribution in the Extended Hand-Arm System at Different Frequencies; (A) 6 Hz; (B) 12 Hz; (C) 38 Hz; (D) 400 Hz.

the shoulder. At higher frequencies (around 400 Hz), small stress is developed around the elbow and palm, while large strain is localized at the palm. Figure 4(a) shows that the highest stress of 23,400 N/m^2 occurred around the shoulder around 8 Hz. The highest strain of 1.28 x 10^{-3} m/m (Figure 4(b)) occurred around the shoulder joint at 12 Hz. Figure 4 shows that stress and strain developed around the shoulder and elbow are high below 20 Hz, while the stress and strain in the palm and wrist are constant in the 2 – 200 Hz range and their values are greater than those developed in the shoulder and elbow above 20 Hz. The trend suggests that low frequency vibration (below 20 Hz) will mostly affect the upper-arm and should while high frequency vibration (above 20 Hz) will mostly affect the fore-arm and the palm.

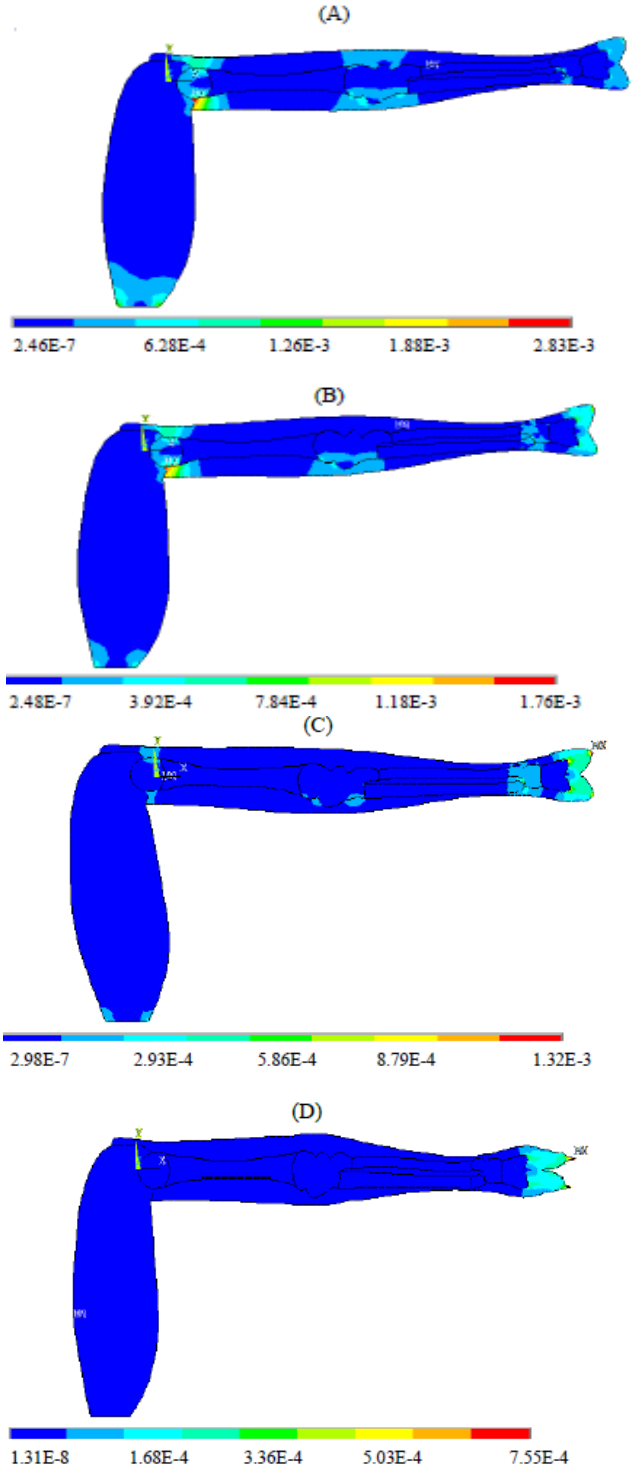

Fig. 3: Strain Distribution in the Extended Hand-Arm System at Different Frequencies; (A) 6 Hz; (B) 12 Hz; (C) 38 Hz; (D) 400 Hz.

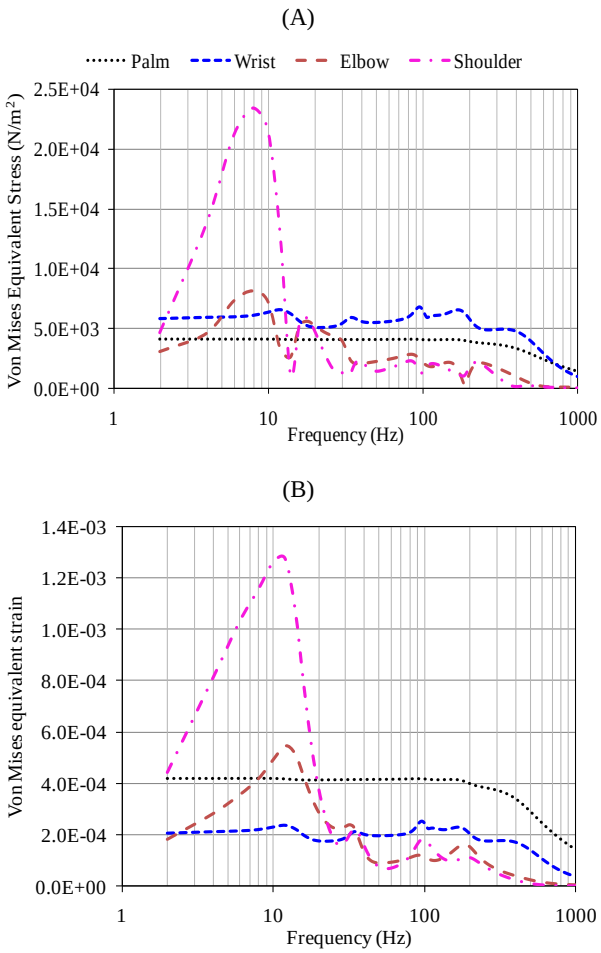

Fig. 4: Stress/Strain Distribution in the Extended Arm Model: (A) Von-Mises Equivalent Stresses; (B) Von-Mises Equivalent Strains

Figures5 and 6 respectively illustrate stress and strain distributions in the bent-arm model, while Figure 7 shows changes in stress and strain calculated at the palm (*X1*), wrist (*X2*), elbow (*X3*) and shoulder (*X4*) on the bent-arm model with frequencies. For the bent-arm model, Figures 5 and 6 show that the general trend of stress and strain distributions is similar to that observed for the extended arm model except that, in addition to the occurrence of the highest stress at the shoulder at 12 Hz, high stress and strain are also developed at 30 Hz around the elbow. Furthermore, high strain occurred at palm in the 2 – 100 Hz frequency range (Figure 7(b)).The values of stress and strain developed in the bent-arm posture are lower than those developed for the extended arm posture. Figure 7 shows that a maximum stress of 16,100 N/m^2 and maximum strain of 8.84 x 10^{-4} m/m occurred at the shoulder at 12 Hz (the corresponding values for the extended arm posture are 23,400 N/m^2 and 1.28 x 10^{-3} m/m around the shoulder at 8 Hz). Unlike the extended arm model, relatively high stress of 11,200 N/m^2 and strain of 7.16 x 10^{-4} m/m also occurred around the elbow at 30 Hz. The maximum stress and strain at the elbow for the extended arm model are 8,160 N/m^2 and 5.46 x 10^{-4} m/m, respectively, at 8 Hz. For the palm, where VWF is observed, the maximum stress and strain are about 5,800 N/m^2 and 4.18 x 10^{-4} m/m for the extended arm in the 2 – 200 Hz range, and 4,930 N/m^2 in the 2 – 200 Hz range and 6.82 x 10^{-4} m/m in the 2 – 50 Hz range for the bent-arm.

The results of stress and strain distributions show that high stress and strain are developed in the extended arm than in the bent-arm, and hence the extended arm posture should be avoided as established by biodynamic responses studies [4, 7, 32]. A recent study on vibration power absorption and hand-arm posture also showed that twice as much power was absorbed in the extended arm posture compared with the bent-arm posture under similar hand forces and excitation conditions [22].

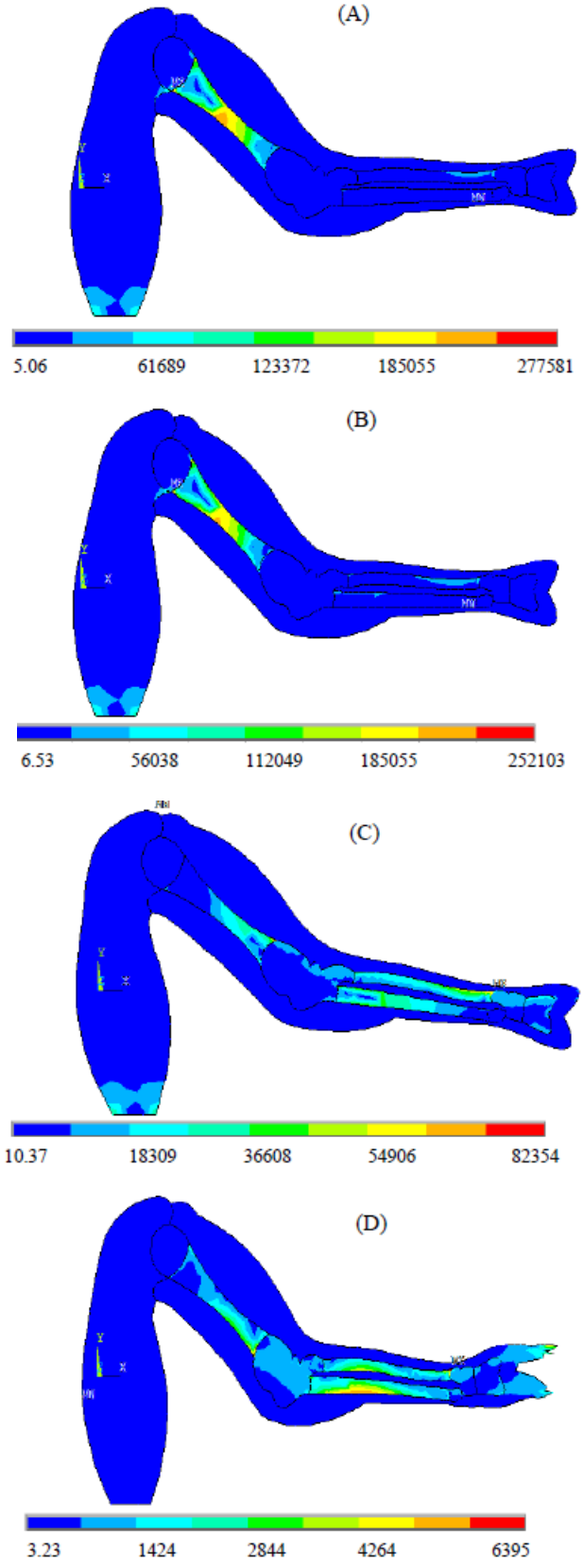

Fig. 5: Stress Distribution in the Bent Hand-Arm System at Different Frequencies; (A) 6 Hz; (B) 12 Hz; (C) 38 Hz; (D) 400 Hz.

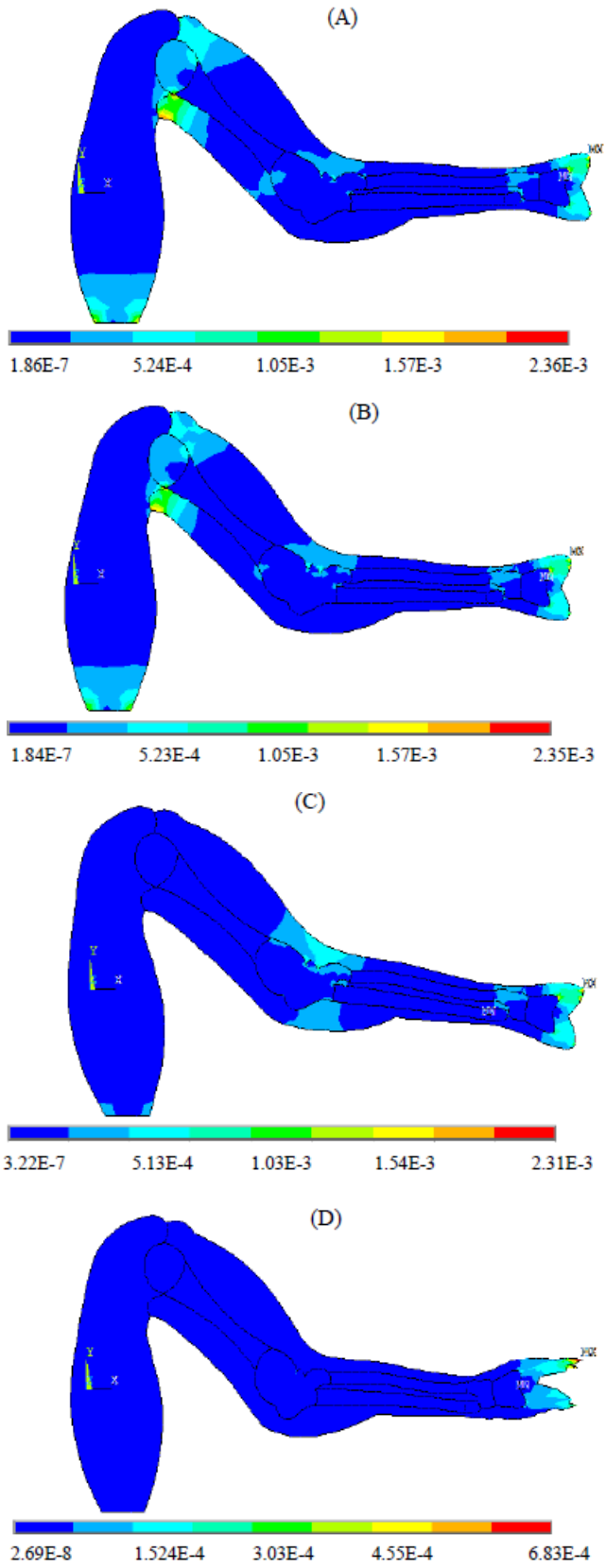

Fig. 6: Strain Distribution in the Bent Hand-Arm System at Different Frequencies; (A) 6 Hz; (B) 12 Hz; (C) 38 Hz; (D) 400 Hz.

Figures 2 - 7 show that as frequency increases, the stress location changes from the upper arm towards the elbow and wrist joints and later confined to the palm at frequencies above 600 Hz. On the other hand, the strain developed at the palm is relatively constant in the 2 – 200 Hz range, while the strain at other locations shifted from the forearm towards the palm with increase in frequency. The strain is confined to the palm at frequency above 600 Hz but strain value decreases above 200 Hz. Injury of the human hand-arm had been associated with vibration-induced deformation, stress and strain, in addition to other factors like cold temperature, obstruction of blood flow, etc. [14, 24].

(A)

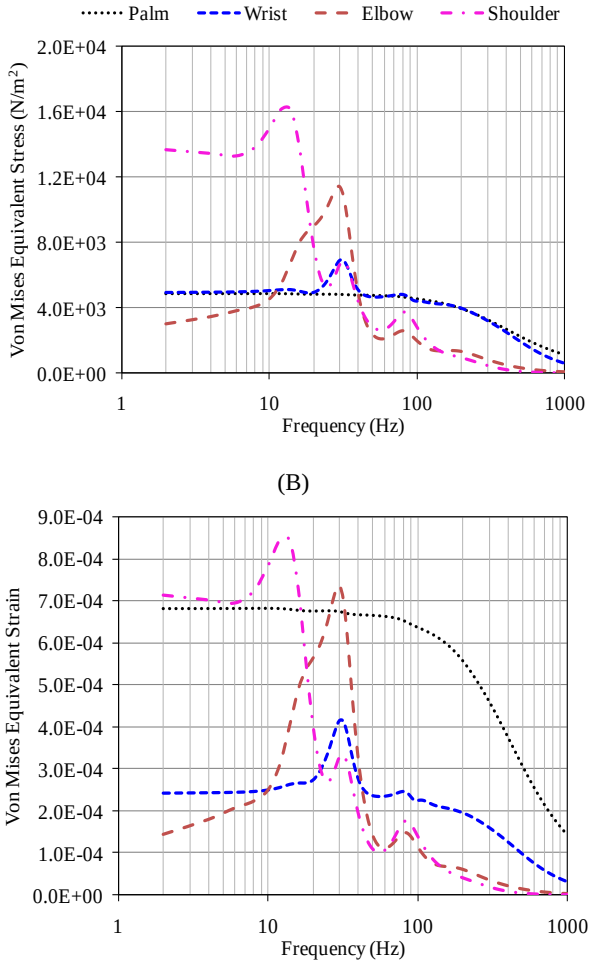

Fig. 7: Stress/Strain Distribution in the Bent-Arm Model :(A) Von-Mises Equivalent Stress; (B) Von-Mises Equivalent Strain.

The results of stress and strain distributions for both the extended arm and bent-arm postures generally showed that high stress, and strain occurred in the upper arm, particularly around the shoulder, at frequencies below 40 Hz. While the stress and strain developed at the palm are higher than those developed in the arms above 40 Hz; however, the values of stress and strain developed in the palm are lower than those developed in the arms, particularly around 12 Hz. Therefore, the results suggest that the frequency weighting recommended in ISO 5349-1 standard [11] may not be suitable for the assessment of the VWF since highest stress and strain around 12 Hz occurred at the shoulder. Furthermore, the occurrence of VWF has also been related to the obstruction of flow of blood in the hand (vasoconstriction), and it has been shown that the highest obstruction of blood flow occurred at frequencies above 63 Hz [14], which is much higher than 12 Hz corresponding to the maximum weight of the frequency weighting reported in ISO 5349-1 [11]. Furthermore, the animation of mode shapes [26 and 27] also showed that the hand-arm system exhibits repeated extension and compression along the z_h-axis at 12.0 Hz. The repeated extension and compression of the hand-arm system around 12 Hz may cause injury of the joints and musculoskeletal disorder. Therefore, vibration around 12 Hz is most unlikely to cause VWF since stresses and strains developed at the palm are higher than those developed at other location only above 40 Hz.

3.2. Stress and strain based frequency weighting

Figure 8 shows the comparison of normalized stress and strain as a function of frequency for the bent-arm model. The figure shows that the trends of normalized stress and strain are similar hence normalized strain distribution alone is considered for subsequent analysis. Figure 9 shows the comparison of the normalized strain with the frequency weightings investigated by Pitts et al. [19]. The main four frequency weightings investigated through the study [19] are: (1) Wh – ISO 5349-1 [11]; (2) W_{hbl} - band-limiting component of W_h (5 – 1200 Hz); (3) W_{hT} – weighting derived by Tominaga [18], which produced better assessment results for vascular injury; and(4) W_{hf}– finger-weighting based on vibration power absorbed in the fingers [20].

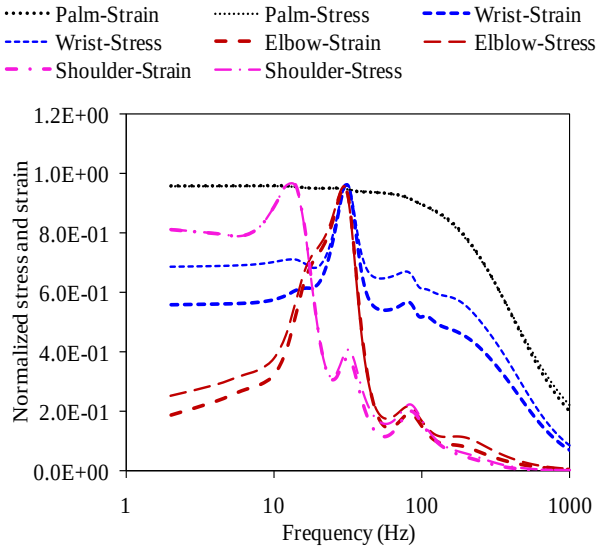

Fig. 8: Comparisons of Normalized Stress And Strain for the Bent-Arm Model.

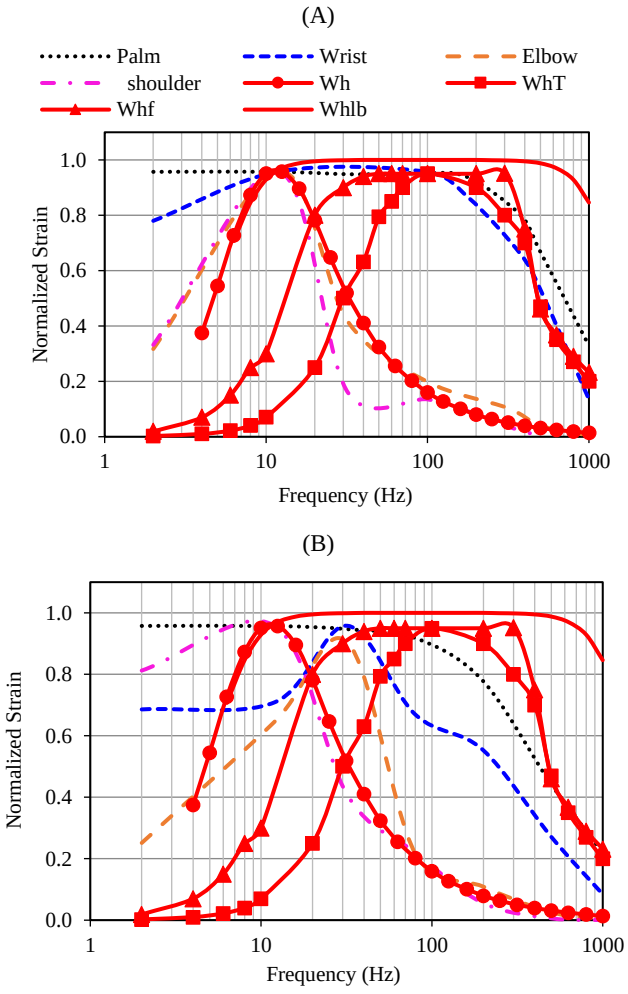

Fig. 9: Comparison of the Stress/Strain-Based Frequency Weightings with ISO [11] and Published Alternative Frequency Weightings; (A) Extended Arm Model; (B) Bent-Arm Model.

For the extended arm model (Figure 9(a)), the strain-based frequency weightings for the elbow and shoulder are comparable with the ISO 5349-1 weighting in the 4 – 1000 Hz range. While the strain-based frequency weightings for the wrist and palm are comparable with W_{hbl} in the 10 -150 Hz frequency range, W_{hf} in the 20 – 1000 Hz range and W_{hT} in the 100 – 1000 Hz frequency range. Similar trends are observed for the bent-arm model except that the strain-based weighting of the wrist is somewhat an outlier with maximum weight occurring at 30 Hz. This suggests that posture of the hand-arm system affects the frequency weighting. Figure 9 clearly shows that the ISO 5349-1 weighting underestimates the potential injury of the hand (VWF) above 20 Hz, since the discrepancy between the strain-based weighting for the palm and ISO 5349-1 weighting increases above 20 Hz. The results of the present study corroborate the results of Thomas and Beauchamp [15] and the study of Bovenzi [13] on the discrepancy in the use of the current ISO 5349-1 frequency weighting for the assessment of VWF. Bovenzi [13] summarized the findings of 25 papers on comparison of VWF prediction based on the ISO weighting with epidemiological studies. The study showed that 33.3% of the papers reported underestimation of VWF risk in workers who operated high speed (high frequency) vibration tools (riveting tools, grinders), while 52.4 % reported that ISO weighting overestimated VWF risk in worker groups exposed to percussive tools (rock drills, road breakers, stone hammers and sand rammers) (low frequency tools), and 14.3 % reported good agreement for forestry workers, snowmobile drivers and stone workers using rotary tools. Furthermore, Figure 9 shows that one single frequency weighting is not sufficient for the assessment of the potential injury risk of hand-transmitted vibration since some hand-held power tools operate at low frequency (2 – 20 Hz), while some operate at high frequency (20 – 200 Hz).

4. Conclusions

Finite-element models of the human hand-arm system in the extended arm and bent-arm postures were used to obtain stress and strain distributions in the hand-arm substructures. Stress- and strain-based frequency weightings at the palm, wrist, elbow and shoulder were derived and compared with frequency weightings available within the literature on the assessment of potential injury of the hand-arm exposed to vibration. There was good correlation between the stress- and strain-based frequency weightings of the shoulder and elbow and ISO 5349-1 [11] frequency weighting. However, huge discrepancy was observed between the stress- and strain-based frequency weightings of the palm and wrist and ISO-5349-1 [11] weighting above 20 Hz. The stress- and strain-based weightings for the palm showed good comparisons with some of the alternative frequency weightings, particularly the weighting derived from vibration power absorbed in the fingers. The results of this study suggest that one frequency weighting is not sufficient to assess the two major components of the hand-arm vibration syndrome (vibration-induced white fingers and musculoskeletal disorder). The current ISO weighting and the stress/strain-based frequency weighting of the shoulder seem appropriate for the assessment of injury risk for musculoskeletal disorder, which is associated with low frequency. The stress/strain-based frequency weighting of the palm seems appropriate for the assessment of potential risk for vibration-induced white finger disorder.

Acknowledgement

The authors acknowledge the financial support from the Natural Science and Engineering Research Council of Canada (NSERC) in the form of Postdoctoral Research Fellowship award to the first author in 2011.

References

[1] M. Bovenzi, L. Petronio and F. DiMarino(1980), Epidemiological survey of shipyard workers exposed to hand-arm vibration. Int. Arch.Occup. Environ. Health46, 251 - 266. https://doi.org/10.1007/BF00380015.

[2] J. Malchaire, B. Maldague, J. M. Huberlant and F. Crouqet (1986), Bone and joint changes in the wrists and elbows and their association with hand and arm vibration exposure. Ann Occup. Hyg 30, 461 – 468.

[3] M. Bovenzi (1998), Exposure-response relationship in the hand–arm vibration syndrome: an overview of current epidemiology research. Int Arch Occup Environ Health, 71, 509–519. https://doi.org/10.1007/s004200050316.

[4] L. Burström(1997), The influence of biodynamic factors on the mechanical impedance of the hand and arm. International Archives of Occupational Environmental Health69, 437– 446. https://doi.org/10.1007/s004200050172.

[5] R. G. Dong, J. H. Dong, J. Z. Wu and S. Rakheja(2007), Modeling of biodynamic responses distributed at the fingers and the palm of the human hand-arm system. Journal of Biomechanics 40, 1335–2340. https://doi.org/10.1016/j.jbiomech.2006.10.031.

[6] Y. Aldien, P. Marcotte, S. Rakheja and P.- É .Boileau(2006), Influence of hand–arm posture on biodynamic response of the hand–arm exposed to z_h-axis vibration. International Journal of Industrial Ergonomics 36, 45 – 59. https://doi.org/10.1016/j.ergon.2005.07.001.

[7] S.A. Adewusi, S. Rakheja, P. Marcotte and J. Boutin(2010, Vibration transmissibility characteristics of the human hand-arm system under different postures, hand forces and excitation levels, Journal of Sound and Vibration329,2953 – 2971. https://doi.org/10.1016/j.jsv.2010.02.001.

[8] X. S. Xu, D. E. Welcome, T. W. McDowell, C. Warren and R. G. Dong (2009), An investigation on characteristics of the vibration transmitted to wrist and elbow in the operation of impact wrenches, International Journal of Industrial Ergonomics 39, 174-184. https://doi.org/10.1016/j.ergon.2008.05.006.

[9] T. Nilsson, L. Burström and M. Hagberg(1989), Risk assessment of vibration exposure and white fingers among platers. Int Arch Occup Environ Health 61, 473 - 481. https://doi.org/10.1007/BF00386482.

[10] J. Starck, P. Jussi and P. Ilmari (1990), Physical characteristics of vibration in relation to vibration-induced white finger. AIHAJ51, 179 – 184. https://doi.org/10.1080/15298669091369510.

[11] International Organization for Standardization ISO 5349-1 (2001), Mechanical vibration and shock– Measurement and evaluation of human ex $\sin x + \cos x = b$. posure to mechanical vibration – part 1: General requirements,

[12] P. L. Pelmear, D. Leong, W. Taylor, M. Nagalingam, D. Fung (1989), Measurement of vibration of hand-held tools: Weighted or unweighted? J.Occup Med 31, 902-908. https://doi.org/10.1097/00043764-198911000-00012.

[13] M. Bovenzi (2012), Epidemiological evidence for new frequency weightings of hand-transmitted vibration. Industrial Health 50 377-387. https://doi.org/10.2486/indhealth.MS1382.

[14] M. Griffin (2012), Frequency-dependence of psychophysical and physiological responses to hand-transmitted vibration. Industrial Health 50, 354-369. https://doi.org/10.2486/indhealth.MS1379.

[15] M. Thomas and Y. Beauchamp (1997), Development of a new frequency weighting filter for the assessment of grinder exposure to wrist-transmitted vibration. Proceedings of the 22nd ICC&IE, Cairo, Egypt, Dec 20-22,4p.

[16] R. G. Dong, D. E. Welcome, T.W. McDowell, J. Z. Wu and A. W. Schopper (2006), Frequency weighting derived from power absorption of fingers-hand-arm system under z_h-axis. Journal of Biomechanics 39, 2311 – 2324. https://doi.org/10.1016/j.jbiomech.2005.07.028.

[17] R. G. Dong, J. Z. Wu, D. E. Welcome, and T. W. McDowell (2008), A discussion on comparing alternative vibration measures with frequency-weighted acceleration defined in ISO standards. Journal of Sound and Vibration317, 1042 – 1050. https://doi.org/10.1016/j.jsv.2008.03.028.

[18] Y. Tominaga (2005), new frequency weighting of hand-arm vibration. Industrial Health43, 509–515. https://doi.org/10.2486/indhealth.43.509.

[19] P. M Pitts, H. J. Mason, K. A. Poole and C. E. Young(2012), Relative performance of frequency weighting W_h and candidates for alternative frequency weightings for predicting the occurrence of hand-transmitted vibration-induced injuries. Industrial Health 50,388 –396. https://doi.org/10.2486/indhealth.MS1381.

[20] J. H. Dong, R. G. Dong, S. Rakheja, D. E. Welcome, T. W. McDowell and J. Z. Wu(2008), A method for analyzing absorbed power distribution in the hand and arm substructures when operating vibration tools. Journal of Sound and Vibration 311, 1286 – 1304. https://doi.org/10.1016/j.jsv.2007.10.031.

[21] S. A. Adewusi, S. Rakheja, and P. Marcotte (2012), Biomechanical Models of the Human Hand-arm to Simulate Distributed Biodynamic Responses for Different Postures. International Journal of Industrial Ergonomics 42,249-260. https://doi.org/10.1016/j.ergon.2012.01.005.

[22] S. Adewusi, S. Rakheja, P. Marcotte and M. Thomas (2013), Distributed vibration power absorption of the human hand-arm system in different postures coupled with vibrating handle and power tools. International Journal of Industrial Ergonomics 43, 363 – 374. https://doi.org/10.1016/j.ergon.2013.04.004.

[23] H. Ayari, M. Thomas, S. Dore and O. Serrus (2009), Evaluation of lumber vertebra injury risk to the seated human body when exposed to vertical vibration. Journal of Sound and Vibration 321 454 – 470. https://doi.org/10.1016/j.jsv.2008.09.046.

[24] J. Z. Wu, R. G. Dong, S. Rakheja, A. W. Schopper (2002), Simulation of mechanical responses of fingertip to dynamic loading. Medical Engineering & Physics 24, 253 – 264. https://doi.org/10.1016/S1350-4533(02)00018-8.

[25] J. Z. Wu, D. E. Welcome, K. Krajnak, R. G. Dong (2007), Finite element analysis of the penetrations of shear and normal vibrations into the soft tissues in a fingertip, Medical Engineering & Physics 29, 718 – 727. https://doi.org/10.1016/j.medengphy.2006.07.005.

[26] S. Adewusi, M. Thomas, V. H. Vu and W. Li (2014**)**, Modal Parameters of the Human Hand-arm using Finite Element and Operational Modal Analysis. Mechanics & Industry, 15(6), 541-549 (DOI: 10.1051/meca/2014060). https://doi.org/10.1051/meca/2014060.

[27] S. Adewusi, M. Thomas and V. H. Vu (2014), Natural Frequencies of the Human Hand-Arm System using Finite Element Method and Experimental Modal Analysis, Transaction on Control and Mechanical Systems, Vol. 3(2), 11-18

[28] International Organization for Standardization ISO 10068 (1998), Mechanical vibration and shock – Mechanical impedance of the human hand-arm system at the driving point.

[29] G. J. LorenandR. L. Lieber (1995), Tendon biomechanical properties enhance wrist muscle specialization, Journal of Biomechanics128, 791 – 799.

[30] C. N. Maganaris and J. P. Paul(1999), In vivo human tendon mechanical properties, Journal of Physiology 521, 307 – 313. https://doi.org/10.1111/j.1469-7793.1999.00307.x.

[31] D. C. Wirtz, T. Schiffers, T. Pandorf, K. Radermacher, D. Weichert and R. Forst (2000), Critical evaluation of known bone material properties to realize anisotropic FE simulation of the proximal femur. Journal of Biomechanics 33, 1325 – 1330. https://doi.org/10.1016/S0021-9290(00)00069-5.

[32] A. J. Besa, F. J. Valero, J.L.Suñer and J. Carballeira (2007), Characterisation of the mechanical impedance of the human hand–arm system: The influence of vibration direction, hand–arm posture and muscle tension. Int. J. of Industrial Ergonomics 37, 225-231. https://doi.org/10.1016/j.ergon.2006.10.019.